Dielectric and piezoelectric properties of $Pb(Ni_{1/3}Nb_{2/3})O_3$–$PbTiO_3$–$PbZrO_3$ ceramics modified with bismuth and zinc substitutions

XINHUA ZHU*
Department of Physics and National Laboratory of Solid State Microstructures, Nanjing University, Nanjing 210093, People's Republic of China

JIE XU, ZHONGYAN MENG
School of Materials Science and Engineering, Shanghai University (Jiading Campus), Shanghai 201800, People's Republic of China

The dielectric and piezoelectric properties of the $(Pb_{0.985}Bi_{0.01})(Ni_{1/4}Zn_{1/12}Nb_{2/3})_x$-$(Zr_\sigma Ti_{1-\sigma})_{1-x}O_3$ piezoelectric ceramic system ($0.2 \leqslant x \leqslant 0.7$, $0.1 \leqslant \sigma \leqslant 0.9$) were systematically investigated. The results showed that, after poling, the dielectric constant, ε_{33}^T, increased for the tetragonal compositions but decreased for the rhombohedral compositions. Furthermore, high values of ε_{33}^T and piezoelectric modulus, d_{31} were found for the compositions along the extension of the morphotropic phase boundary. The highest values of the planar electromechanical coupling factor, K_p, and the piezoelectric modulus, d_{31}, were found to be 0.70 and -274×10^{-12} C N^{-1}, respectively. The Curie temperature, remanent polarization, coercive field and the lattice constants of the *a* and *c* axes in relation to the $Pb(Ni_{1/3}Nb_{2/3})O_3$ content and the $Zr/Zr + Ti$ ratio were also determined.

1. Introduction

Since Jaffe [1] discovered that the poled lead zirconate titanate (PZT) ceramics with compositions near the phase boundary between the rhombohedral and tetragonal ferroelectric phases (MPB), exhibited high piezoelectric activity and dielectric constants, PZT ceramics have been widely used to produce piezoelectric devices [2–4]. In order to reach the requirements of practical applications, a number of minor additives have been added to modify the piezoelectric properties of the PZT ceramics [5–7]. However, when two or more minor additives were added simultaneously, the piezoelectric properties obtained were not greatly improved. Therefore, the ternary solid solution in the PZT-based ceramics with the perovskite structure was synthesized; its formation has been widely used to improve piezoelectric properties [8–10].

In this work, the ternary system $Pb(Ni_{1/3}Nb_{2/3})O_3$–$PbZrO_3$–$PbTiO_3$ (PNN-PZ-PT) was chosen, and modified with bismuth and zinc substitutions to obtain suitable materials for fabricating ceramic actuators, such as the piezoelectric actuator prepared with functionally gradient materials (FGM; the structure and operational principles of these are presented elsewhere [11]). Because the piezoelectric motion employed in the FGM actuator is a longitudinal mode for the thin plate, to obtain a high strain, it is very desirable that the materials of the piezoelectric layer within the FGM actuator possess a high piezoelectric strain modulus, d_{31}, and also maintain a fairly high coercive field to prevent depolarization occurring when the FGM actuator is operated at high electric field. In dielectric materials, high dielectric constant and low piezoelectric modulus are required to construct high gradients of the electric properties with the piezoelectric materials. In order to choose suitable materials whose electric properties can reach the above requirements for fabricating the FGM piezoelectric actuator, it is necessary to investigate the dielectric and piezoelectric properties of the PNN–PZ–PT ternary system modified with bismuth and zinc substitutions. Kitamura *et al.* [12] investigated the effects of the addition of bismuth and zinc on the dielectric and piezoelectric properties of the ternary system, and found that the piezoelectric activity and temperature stability could be improved. However, no detailed investigations have been made on the relationship between the compositions and the electrical (dielectric and piezoelectric) properties of the PNN–PN–PT system modified with bismuth and zinc substitutions. The dependence of the dielectric and piezoelectric properties on the compositions, especially around the MPB in such a solid solution, is of a great interest both theoretically and for practical

* Author to whom correspondence should be addressed

0022–2461

applications. Therefore, the main purpose of the present study was to investigate systematically the dielectric and piezoelectric properties of the $(Pb_{0.985}Bi_{0.01})$-$(Ni_{1/4}Zn_{1/12}Nb_{2/3})_x(Zr_\sigma Ti_{1-\sigma})_{1-x}O$ ceramic system ($0.2 \leqslant x \leqslant 0.7$, $0.1 \leqslant \sigma \leqslant 0.9$), with emphasis on the influence of the MPB on the dielectric and piezoelectric properties.

2. Experimental procedure

The compositions used in this study were $(Pb_{0.985}Bi_{0.01})(Ni_{1/4}Zn_{1/12}Nb_{2/3})_x(Zr_\sigma Ti_{1-\sigma})_{1-x}O_3$ ($0.2 \leqslant x \leqslant 0.7$, $0.1 \leqslant \sigma \leqslant 0.9$), whose positions in the phase diagram of the PNN–PZ–PT ternary system are shown in Fig. 1. The substitution of lead with bismuth atoms was in stoichiometric proportions, $Pb_{1-3\alpha/2}Bi_\alpha$ with $\alpha = 0.01$, and zinc substituting nickel atoms on a 25 mol % scale. The method of preparing the samples was described elsewhere [13]. Two types of the sample were fabricated: discs (diameter = 20 mm) and rectangular plates ($25 \times 4 \times 1.0\,mm^3$). The samples were sintered at temperatures between 1220 and 1260 °C, and for sintering times from 1–3 h. To determine the lattice parameters, the sintered samples were analysed by XRD (D/max-C, Rigaku, Tokyo, Japan). The samples were polished and electroded with silver paste. Before poling, the dielectric constant at room temperature was measured, and compared with that of the poled samples, which were poled at 100–120 °C in a silicone oil bath for 30 min under a d.c. field of $4\,V\,mm^{-1}$. The Curie temperature was determined from the temperature dependence of the dielectric constant, ε_{33}^T, measured at 1 kHz with HP4112A. At room temperature, the polarization, P, versus the electric field, E, hysteresis loop was measured at 0.2 Hz using a modified Sawyer–Tower circuit. The electromechanical planar coupling factor, K_p, piezoelectric modulus, d_{31}, and elastic constant, s_{11}^E, were calculated using the resonance and anti-resonance frequencies.

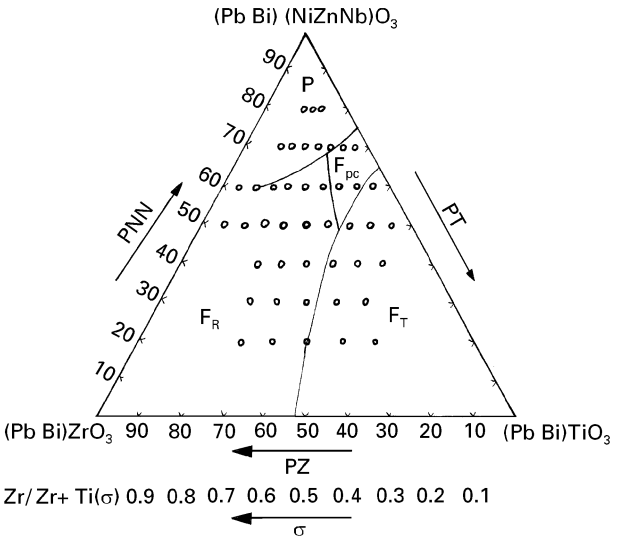

Figure 1 The compositions used in this study and their positions in the phase diagram of the PNN–PZ–PT ternary system modified with bismuth and zinc substitutions.

3. Results and discussion

3.1. Dielectric properties

In piezoelectric ceramics, the dielectric properties depend on the composition and crystal structure; the dielectric constant may be decreased or increased by the poling treatment. The variations of dielectric constants, ε_{33}^T, at room temperature and $f = 1$ kHz with compositions $(Pb_{0.985}Bi_{0.01})(Ni_{1/4}Zn_{1/12}Nb_{2/3})_x$-$(Zr_\sigma Ti_{1-\sigma})_{1-x}O_3$ of the piezoelectric ceramic system ($0.2 \leqslant x \leqslant 0.7$, $0.1 \leqslant \sigma \leqslant 0.9$) ceramics, before and after poling, are shown in Fig. 2a and b, respectively. By comparing Fig. 2a with Fig. 2b, it can be seen that the dielectric constant, ε_{33}^T, before poling is slightly higher than that after poling in the rhombohedral phase region. This phenomenon changes along the phase boundary between the rhombohedral and tetragonal phases, and then, after poling, ε_{33}^T becomes slightly higher than that before poling in the tetragonal phase region. The difference in dielectric constant, ε_{33}^T, before poling and after poling is determined by two factors. The first is the variation in the direction of the polar axis in the crystal for non-180° domain orientations, resulting in a decrease in the dielectric constant because of the dielectric anisotropy. The second factor is that the "clamping" effect

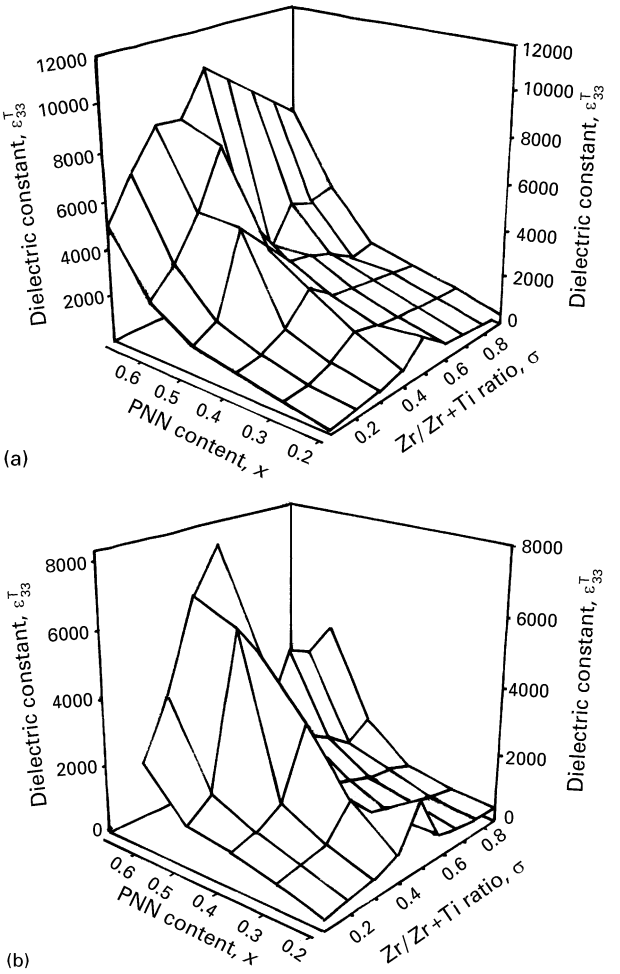

Figure 2 The dielectric constant ε_{33}^T, at room temperature for the compositions of the $(Pb_{0.985}Bi_{0.01})(Ni_{1/4}Zn_{1/12}Nb_{2/3})_x(Zr_\sigma Ti_{1-\sigma})_{1-x}O_3$ ceramic system ($f = 1$ kHz): (a) before poling, $f = 1$ kHz; (b) after poling, d.c. $40\,kV\,cm^{-1}$, $f = 1$ kHz.

of 180° domain orientation is removed in a poled ceramic, due to the complete 180° domain switching, which increases the dielectric constant. When poling the tetragonal compositions, the increase in the dielectric constant can be interpreted as being due to the elimination of the effect of compression of the 180° domains. For the rhombohedral compositions, the decrease in the dielectric constant after poling is attributed to the 90° domain reorientation which dominates the effect of the removal of compression, and causes the dielectric anisotropy. In the region of the morphotropic phase boundary (between the rhombohedral and tetragonal phases), the dielectric constant had the highest value. which was attributed to the oscillations of the boundaries of the co-existing phases [14]. On increasing the PNN content from 20 mol % to 50 mol % the ratio of zirconium to (Zr + Ti), corresponding to the maximum of the dielectric constant, ε_{33}^{T}, decreases from 0.5 to 0.3. This implies that the phase boundary existing between the tetragonal and rhombohedral phases becomes closer to the $PbTiO_3$ side with increasing the PNN content. When the PNN molar content is equal to 0.6, the compositions of the $(Pb_{0.985}Bi_{0.01})(Ni_{1/4}Zn_{1/12}Nb_{2/3})_{0.6}(Zr_{\sigma}Ti_{1-\sigma})_{0.4}O_3$ system cross three phase boundaries as the Zr/Zr + Ti ratio varies; these are the phase boundaries between the rhombohedral and pseudocubic phases, the tetragonal and pseudocubic phases, the rhombohedral and paraelectric phases. The compositions close to the phase boundary between the rhombohedral and pseudocubic phases yield the highest dielectric constant. When the Zr/Zr + Ti ratio is constant, after poling, the dielectric constant, ε_{33}^{T}, at room temperature and $f = 1$ kHz,

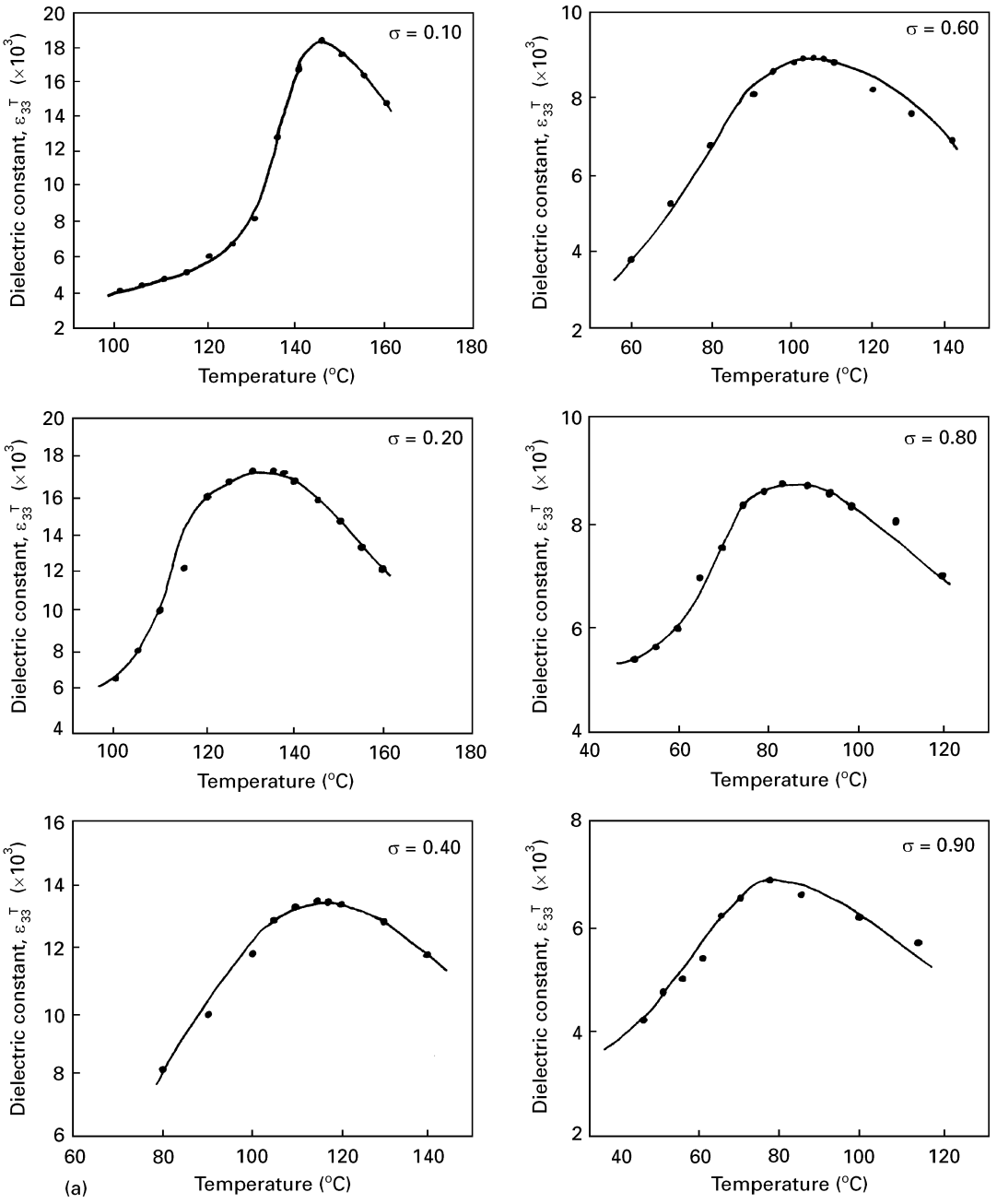

Figure 3 The dielectric constant, ε_{33}^{T}, versus the temperature measured at $f = 1$ kHz for the compositions (a) $(Pb_{0.985}Bi_{0.01})(Ni_{1/4}Zn_{1/12}Nb_{2/3})_{0.6}(Zr_{\sigma}Ti_{1-\sigma})_{0.4}O_3$ and (b) $Pb_{0.985}Bi_{0.01})(Ni_{1/4}\ Zn_{1/12}Nb_{2/3})_x(Zr_{0.6}Ti_{0.4})_{1-x}O_3$.

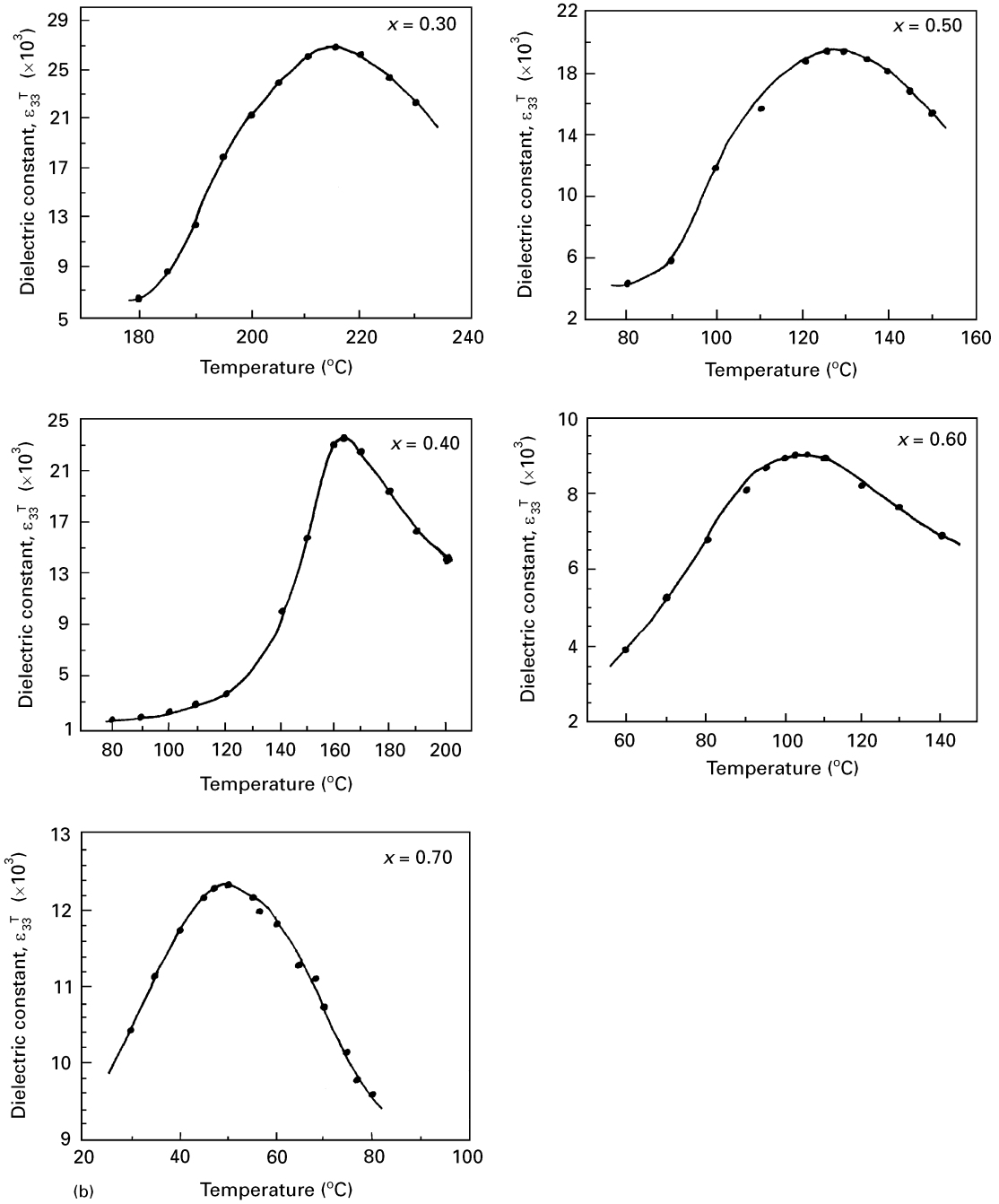

Figure 3 Continued.

increases monotonically with increasing the PNN content from 30 mol % to 60 mol %. Furthermore, the increment ratio is also increased. This phenomenon can be interpreted from the decrease in Curie temperature T_c towards room temperature with increasing the PNN content. In addition, the rate of shift of the Curie temperature increases with increasing the PNN content. Therefore, the peak value of the dielectric constant corresponding to the Curie temperature becomes close to that at room temperature and the increment ratio of the dielectric constant is enhanced.

3.2. Curie temperature

The Curie temperatures for PNN, PZ and PT are −120, 230 and 490 °C, respectively. It is expected that the Curie temperature of the PNN–PZ–PT system, modified with bismuth and zinc substitutions, can be

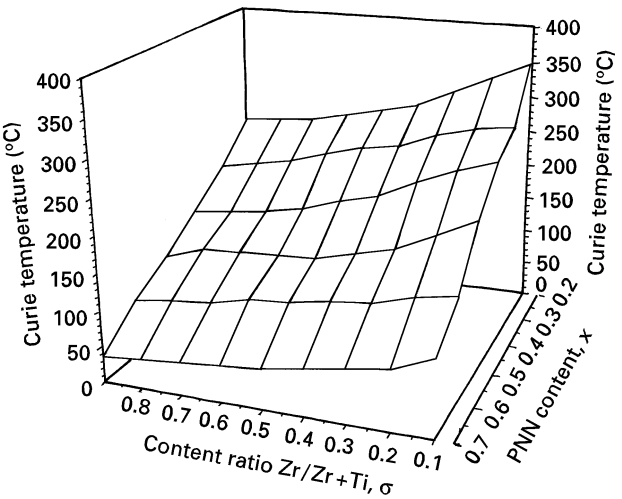

Figure 4 Curie temperature versus the PNN content and the Zr to Zr + Ti ratio.

designed by controlling the compositions. The Curie temperatures for the compositions of the $(Pb_{0.985}Bi_{0.01})(Ni_{1/4}Zn_{1/12}Nb_{2/3})_{0.6}(Zr_{\sigma}Ti_{1-\sigma})_{0.4}O_3$ system were obtained from the dependence of the dielectric constants, ε_{33}^{T}, on the temperature measured at 1 kHz, as shown in Fig. 3a. Similarly, the Curie temperature for the compositions of the $(Pb_{0.985}Bi_{0.01})(Ni_{1/4}Zn_{1/12}Nb_{2/3})_x(Zr_{0.4}Ti_{0.6})_{1-x}O_3$ system can be obtained from Fig. 3b. The dependences of the Curie temperature for the $(Pb_{0.985}Bi_{0.01})(Ni_{1/4}Zn_{1/12}Nb_{2/3})_x(Zr_{\sigma}Ti_{1-\sigma})_{1-x}O_3$ system on the PNN content and the Zr/Zr + Ti ratio are illustrated in Fig. 4. When the PNN content is constant the Curie temperature varies almost linearly with the ratio of Zr to Zr + Ti, and a similar phenomenon occurs for the Curie temperature versus the PNN content when the Zr/Zr + Ti is constant. Because the nickel atoms of $Pb(Ni_{1/3}Nb_{2/3})O_3$ are partially subsitituted by zinc atoms and the Curie temperature for $Pb(Zn_{1/3}Nb_{2/3})O_3$ ($T_c = 140\,^{\circ}C$) is much higher than that of $Pb(Ni_{1/3}Nb_{2/3})O_3$, the Curie temperature for the $(Pb_{0.985}Bi_{0.01})(Ni_{1/4}Zn_{1/12}Nb_{2/3})_x(Zr_{\sigma}Ti_{1-\sigma})_{1-x}O_3$ system decreased much more slowly with increasing PNN content when the ratio of Zr to Zr + Ti was constant. By suitably controlling the PNN content and the Zr/Zr + Ti ratio, the Curie temperature of the ternary system can be adjusted to

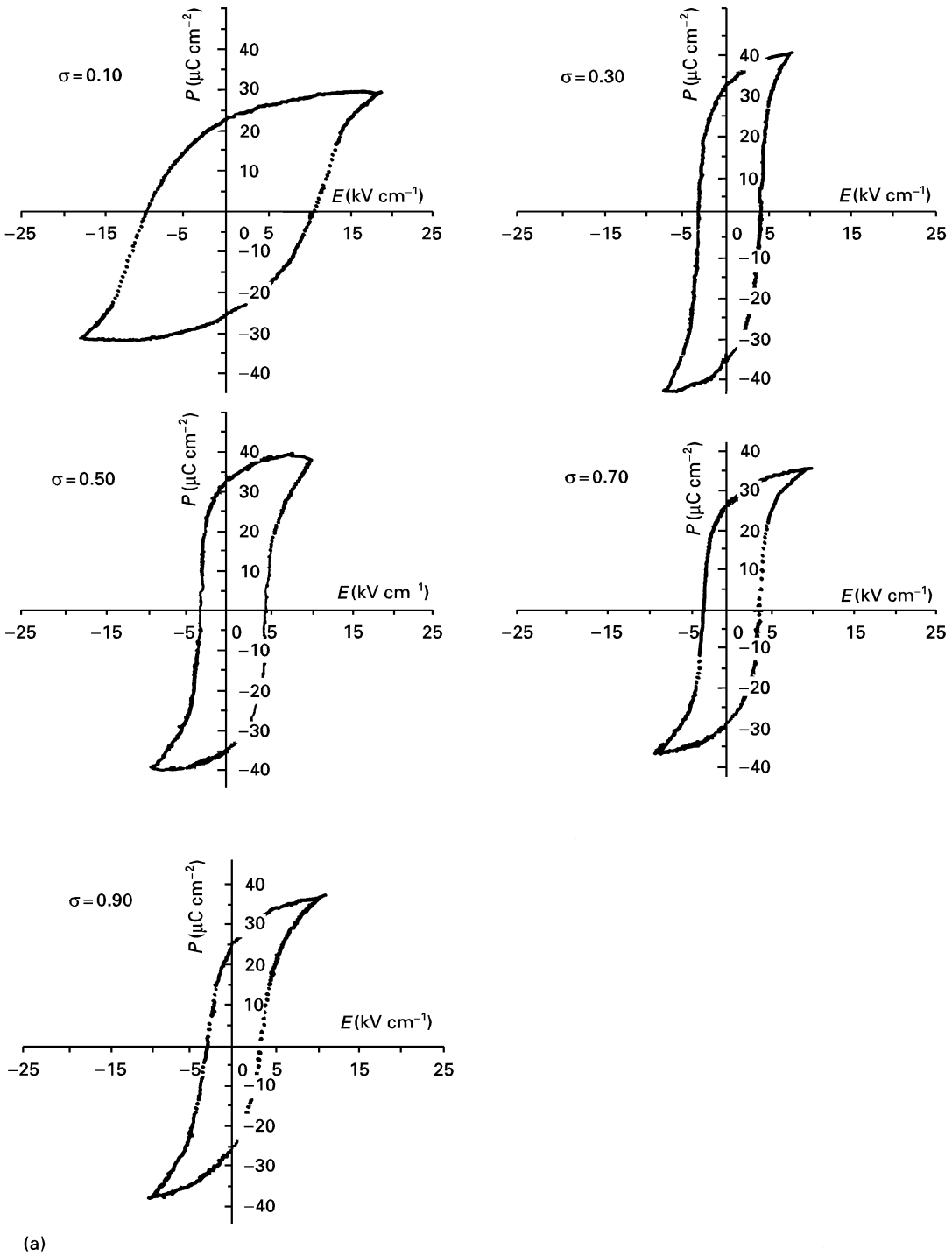

Figure 5 The polarization versus the electric field characteristics for the compositions of (a) $(Pb_{0.985}Bi_{0.01})(Ni_{1/4}Zn_{1/12}Nb_{2/3})_{0.5}(Zr_{\sigma}Ti_{1-\sigma})_{0.5}O_3$ and (b) $(Pb_{0.985}Bi_{0.01})(Ni_{1/4}Zn_{1/12}Nb_{2/3})_x(Zr_{0.3}Ti_{0.7})_{1-x}O_3$.

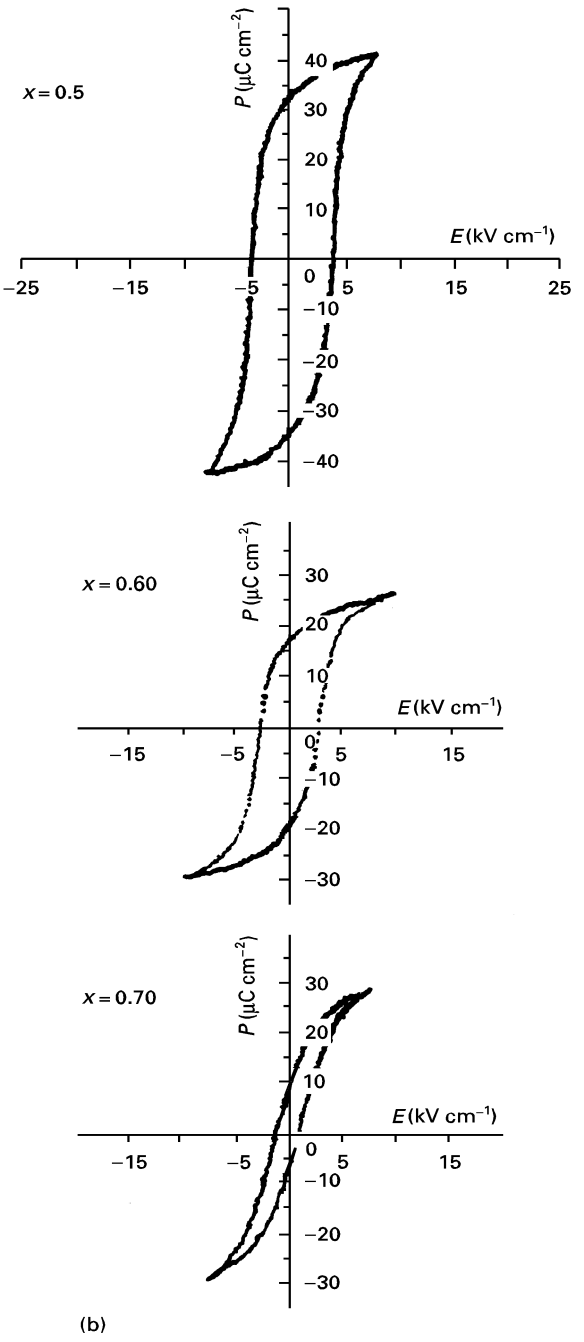

Figure 5 Continued.

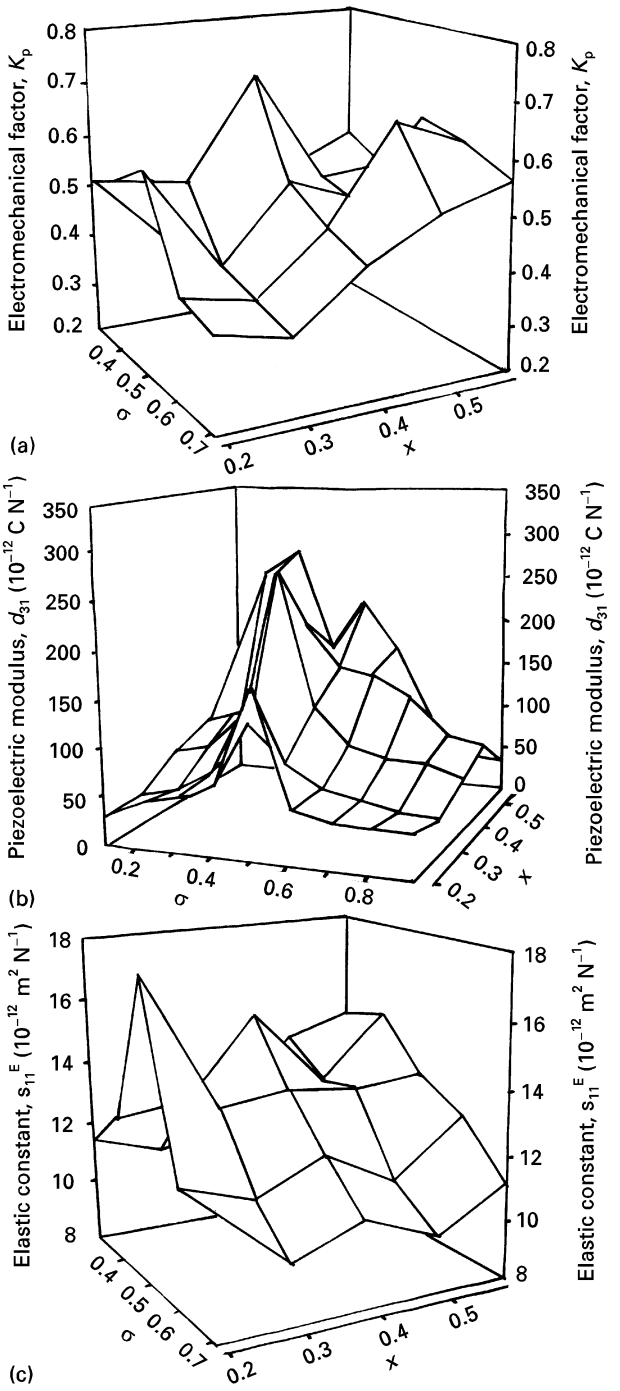

Figure 6 (a) The electromechanical cooling factor, K_p, (b) piezoelectric modulus, d_{31}, and (c) elastic constant, s_{11}^E, versus the PNN content and the Zr to Zr + Ti ratio.

make the dielectric constant reach the requirements of practical applications.

3.3. Remanent polarization and coercivity

The typical polarization versus electric field characteristics for the $(Pb_{0.985}Bi_{0.01})(Ni_{1/4}Zn_{1/12}Nb_{2/3})_{0.5}$-$(Zr_\sigma Ti_{1-\sigma})_{0.5}O_3$ $(0.1 \leqslant \sigma \leqslant 0.9)$ and $(Pb_{0.985}Bi_{0.01})$-$(Ni_{1/4}Zn_{1/12}Nb_{2/3})_x(Zr_{0.3}Ti_{0.7})_{1-x}O_3$ systems $(0.5 \leqslant x \leqslant 0.7)$ are shown in Fig. 5a and b, respectively. In Fig. 5a it is observed that the remanent polarization for the composition ($x = 0.50$, $\sigma = 0.30$) near the MPB exhibited a maximum, which was attributed to the dipole moments of the compositions near the MPB being able to reorientate themselves more completely than those of the rhombohedral or tetragonal phases. It is well known that the polarization vector of the rhombohedral phase is $\langle 1\,1\,1 \rangle$ and has eight directions for dipole moment reorientation. Similarly the polarization vector is $\langle 0\,0\,1 \rangle$ for the tetragonal phase and has six directions for dipole moment reorientation. Because of the compositions of the rhombohedral and tetragonal phases coexisting at the MPB, there are fourteen directions for dipole moment reorientation. Thus the remanent polarization of the composition near the MPB is higher than that of the tetragonal or rhombohedral phases. The coercivities of the rhombohedral and cubic phases are lower than that of the tetragonal phase, as shown in Fig. 6. When the Zr/Zr + Ti ratio was increased, the phase structure transformed from the tetragonal to the rhombohedral

or cubic phases, resulting in the decreasing coercivity. This result is shown in Fig. 5a. In addition, with increasing PNN content, the crystal structure becomes closer to the cubic phase, which also causes the coercive field to decrease, as illustrated in Fig. 5b.

3.4. Piezoelectric properties

The varations of the electromechanical coupling factor, K_p, piezoelectric modulus, d_{31}, and elastic constant s_{11}^E, with the PNN content and the Zr/Zr + Ti ratio are shown in Fig. 6a, b and c, respectively. In the MPB region, the piezoelectric coeffcients had the highest values. The highest electromechanical coupling factor, K_p, was found to be 0.70 for the composition $(Pb_{0.985}Bi_{0.01})(Ni_{1/4}Zn_{1/12}Nb_{2/3})_{0.4}$-$(Zr_{0.4}Ti_{0.6})_{0.6}O_3$ with the highest piezoelectric modulus $d_{31} = -274 \times 10^{-12}$ C N^{-1} and the elastic constant $s_{11}^E = 15.57 \times 10^{-12}$m^2 N^{-1}. Because the structural activities for the compositions near the MPB region are high, phase transition from the rhombohedral ferroelectric phase to the tetragonal phase, accompanied by mobility and polarization of ions, can occur easily. Such structural transition is very beneficial in enhancing the piezoelectric properties, and vice versa. Because the lead and nickel ions are partially substituted with bismuth and zinc ions respectively, the components of the A and B sites within the perovskite structure become more complex, which may cause the unit cell to become softer and may enhance the elasticities of materials.

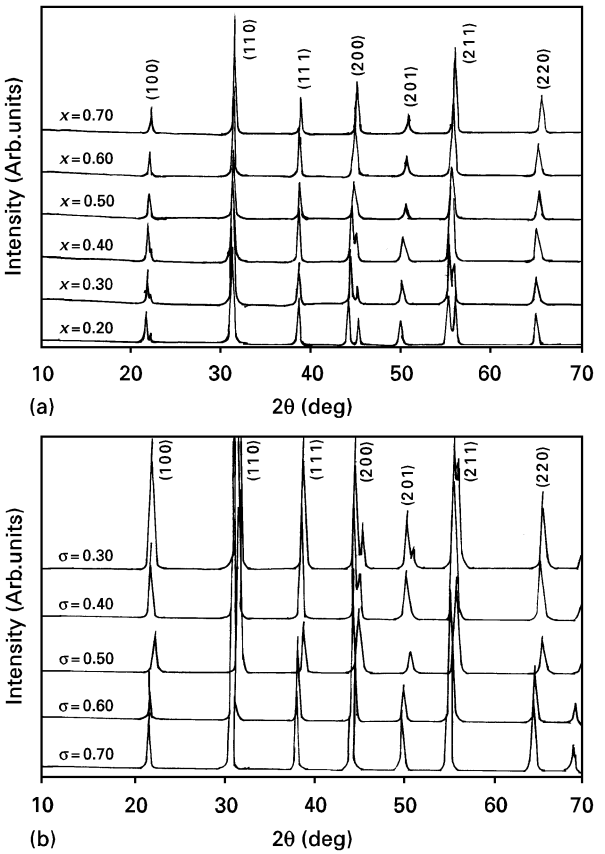

Figure 7 XRD patterns for the compositions $(Pb_{0.985}Bi_{0.01})$-$(Ni_{1/4}Zn_{1/12}Nb_{2/3})_x(Zr_\sigma Ti_{1-\sigma})_{1-x}O_3$ for (a) $\sigma = 0.40$, (b) $x = 0.40$.

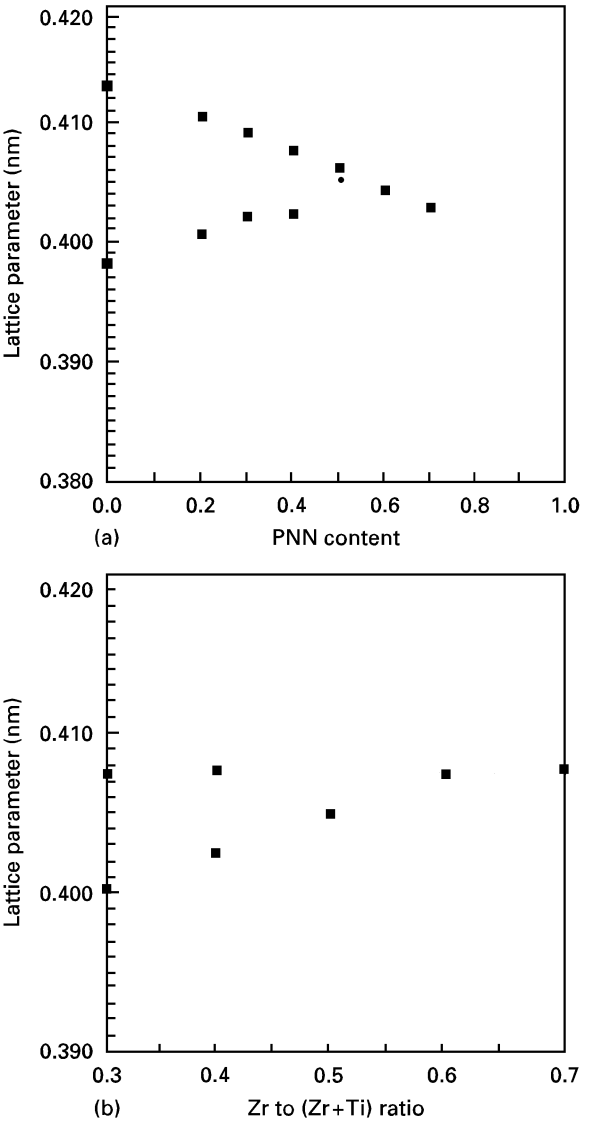

Figure 8 Lattice constants of the compositions $(Pb_{0.985}Bi_{0.01})$-$(Ni_{1/4}Zn_{1/12}Nb_{2/3})_x(Zr_\sigma Ti_{1-\sigma})_{1-x}O_3$ determined from XRD, versus the PNN content and the Zr to Zr + Ti ratio: (a) $\sigma = 0.40$, (b) $x = 0.40$.

3.5. Lattice constants

XRD patterns for the compositions of the $(Pb_{0.985}$-$Bi_{0.01})(Ni_{1/4}Zn_{1/12}Nb_{2/3})_x(Zr_{0.4}Ti_{0.6})_{1-x}O_3$ and $(Pb_{0.985}$-$Bi_{0.01})(Ni_{1/4}Zn_{1/12}Nb_{2/3})_{0.4}(Zr_\sigma Ti_{1-\sigma})_{0.6}O_3$ systems are shown in Fig. 7a and b, respectively. The lattice constants determined from XRD patterns are shown in Fig. 8a and b, respectively. The lattice constant of the *a*-axis increased with increasing PNN content, whereas the lattice constant of the *c*-axis decreased when the Zr/Zr + Ti was constant (e.g. equal to 0.40). A similar phenomenon occurred for the lattice constants of the *a*- and *c*-axes versus the Zr/Zr + Ti ratio when the PNN content was constant. The variations of the lattice constants resulted from the structural phase transition from the tetragonal to rhombohedral phases with increasing PNN content or the Zr/Zr + Ti ratio.

4. Conclusions

The dielectric and piezoelectric properties of the $(Pb_{0.985}Bi_{0.01})(Ni_{1/4}Zn_{1/12}Nb_{2/3})_x(Zr_\sigma Ti_{1-\sigma})_{1-x}O_3$

piezoelectric system were investigated. The compositions near the MPB yield the highest dielectric and piezoelectric properties. The highest planar coupling factor K_p, was found to be 0.70 and d_{31} to be -274×10^{-12} C N^{-1}. The Curie temperature varied almost linearly with the PNN content and the Zr/Zr + Ti ratio. The lattice constant of the *a*-axis increased with increasing PNN content or the Zr/Zr + Ti ratio, whereas the reverse variations occurred for the lattice constant of the *c*-axis.

Acknowledgement

The authors acknowledge the financial support for this project by the National Natural Science Foundation of China, grant no. 59 282 018.

References

1. B. JAFFE, W. R. COOK and H. JAFFE, "Piezoelectric ceramics" (Academic press, London, 1971).
2. M. ADACHI, A. HACHISUKA, N. OKUMURA, T. SHIOSAKI and A. KAWABATA, *Jpn. J. Appl. Phys.* **29** (1987) 68.
3. W. P. ROBBINS, D. L. POLLA and D. E. GLUMAC, *IEEE Trans. Ultrason. Ferroelec. Feq. Contr.* **38** (1991) 454.
4. L. JONTS, E. GARCIA and H. WAITES, *Smart. Mater. Struct.* **3** (1994) 147.
5. R. GERSON, *J. Appl. Phys.* **31** (1960) 188.
6. F. KULCSAR, *J. Amer. Ceram. Soc.* **42** (1959) 343.
7. M. TAKAHASHI, *Jpn J App. Phys.* **9** (1970) 1236.
8. H. OUCHI, *J. Amer. Ceram. Soc.* **51** (1968) 169.
9. H. OUCHI, K. NAGANO and S. HAYAKAWA, *ibid.* **48** (1965) 630.
10. J. H. MOON and H. M. JANG, *J Mater. Res.* **8** (1993) 3184.
11. X. H. ZHU and Z. Y. MENG, *Sensors Actuators A Physical* **48** (3) (1995) 169.
12. T. KITAMURA, Y. KODERA, K. MIYAKARA and H. TAMURA, *Jpn. J. Appl. Phys.* **20** (1981) 97.
13. X. H. ZHU and Z. Y. MENG, *J. Mater. Sci.* **31** (1996) 2171.
14. M. J. HAUN, E. FURMAN, S. J. JANG and L. E. CROSS, *Ferroelectrics* **99** (1989) 13.

Received 3 May 1996
and accepted 28 January 1997